CONDENSED MATTER PHYSICS

Ultrafast time-resolved x-ray scattering reveals diffusive charge order dynamics in La$_{2-x}$Ba$_x$CuO$_4$

Matteo Mitrano[1,2]*, Sangjun Lee[1,2], Ali A. Husain[1,2], Luca Delacretaz[3], Minhui Zhu[1], Gilberto de la Peña Munoz[4], Stella X.-L. Sun[1,2], Young Il Joe[5], Alexander H. Reid[4], Scott F. Wandel[4†], Giacomo Coslovich[4], William Schlotter[4], Tim van Driel[4], John Schneeloch[6‡], G. D. Gu[6], Sean Hartnoll[3], Nigel Goldenfeld[1]*, Peter Abbamonte[1,2]*

Charge order is universal among high-T_c cuprates, but its relation to superconductivity is unclear. While static order competes with superconductivity, dynamic order may be favorable and even contribute to Cooper pairing. Using time-resolved resonant soft x-ray scattering at a free-electron laser, we show that the charge order in prototypical La$_{2-x}$Ba$_x$CuO$_4$ exhibits transverse fluctuations at picosecond time scales. These sub–millielectron volt excitations propagate by Brownian-like diffusion and have an energy scale remarkably close to the superconducting T_c. At sub–millielectron volt energy scales, the dynamics are governed by universal scaling laws defined by the propagation of topological defects. Our results show that charge order in La$_{2-x}$Ba$_x$CuO$_4$ exhibits dynamics favorable to the in-plane superconducting tunneling and establish time-resolved x-rays as a means to study excitations at energy scales inaccessible to conventional scattering techniques.

INTRODUCTION

One of the key questions in high-temperature superconductivity is how it emerges as hole-like carriers are added to a correlated Mott insulator (1–3). Soon after the discovery of Bednorz and Müller (4), it was recognized that competition between kinetic energy and Coulomb repulsion could cause valence holes to segregate into periodic structures originally referred to as "stripes" (5–7). Valence band charge order has since been observed in nearly all cuprate families (8–19), although it is not known what role, if any, charge order plays in superconductivity.

It is widely believed that, while static charge order may compete with superconductivity, fluctuating order could be favorable or even contribute to the pairing mechanism (1, 2, 20). For example, transverse stripe fluctuations have been cited as a means to enhance superconductivity by modulating the interstripe Josephson coupling (1, 21). It is therefore crucial to determine whether the charge order in cuprates is fluctuating and, if so, what kind of dynamics it exhibits.

The generally accepted way to detect fluctuating charge order is to use energy- and momentum-resolved scattering techniques, such as inelastic x-ray or electron scattering, to measure the dynamic structure factor, $S(q, \omega)$ (2, 20). This quantity is related to the charge susceptibility, $\chi''(q, \omega)$, by the fluctuation-dissipation theorem, which asserts a quantitative relationship between the weakly nonequilibrium dynamics of a system and its equilibrium fluctuations at finite temperature (22–25). The time scale of the fluctuations can therefore be inferred from the energy dependence of the scattering data. The energy scale of charge fluctuations could, however, be of the same order as the

superconducting gap, requiring instruments with sub–millielectron volt energy resolution to detect it. These x-ray and electron spectrometers do not yet exist, calling for a different approach.

An alternative way to achieve sub–millielectron volt energy resolution is to study the collective excitations in the time domain. The effective energy resolution of a time-resolved experiment can be defined as $\Delta\omega = 2\pi\hbar/t_d$, where t_d is the time interval measured (26). Arbitrarily low energy scales can therefore be accessed by scanning to long delay times. Furthermore, the fluctuation-dissipation theorem guarantees that the time-domain dynamics of a system may be used to shed light on its low-energy fluctuations in equilibrium.

When an ordered phase is excited out of equilibrium, its order parameter could exhibit any of several distinct types of dynamics (23–25). For example, it might exhibit inertial dynamics, undergoing coherent oscillation around its equilibrium value at a characteristic frequency. These dynamics are common in structural phase transitions in which the oscillation is a phonon of the distorted phase. Alternatively, the order parameter might relax back to equilibrium gradually, through either dissipation or diffusive motion of excitations. This relaxation is influenced by conservation laws and by the possible presence of continuous symmetries that support topological defects (24, 25). Recent time-resolved optics studies of underdoped YBa$_2$Cu$_3$O$_{6+x}$ and La$_{2-x}$Sr$_x$CuO$_4$ showed coherent, millielectron volt–scale oscillations that were interpreted as an amplitude mode of the charge order (27–29), implying that the charge dynamics are inertial (24, 25). However, optics experiments probe the system at zero momentum and are not selectively sensitive to charge order, which is an innately finite-momentum phenomenon. Hence, momentum-resolved techniques capable of directly studying the microscopic dynamics of the charge order are greatly needed.

RESULTS AND DISCUSSION

Here, we use time-resolved resonant soft x-ray scattering (tr-RSXS) to study the collective dynamics of "stripe-ordered" La$_{2-x}$Ba$_x$CuO$_4$ with $x \sim 1/8$ (LBCO) (8, 9, 30). We use 50-fs, 1.55-eV laser pulses to drive the charge order parameter out of equilibrium and probe its subsequent dynamics by scattering 60-fs x-ray pulses from a free-electron

[1]Department of Physics, University of Illinois at Urbana-Champaign, Urbana, IL 61801, USA. [2]Seitz Materials Research Laboratory, University of Illinois at Urbana-Champaign, Urbana, IL 61801, USA. [3]Department of Physics, Stanford University, Stanford, CA 94305-4060, USA. [4]SLAC National Accelerator Laboratory, 2575 Sand Hill Road, Menlo Park, CA 94025, USA. [5]National Institute of Standards and Technology, Boulder, CO 80305, USA. [6]Condensed Matter Physics and Materials Science Department, Brookhaven National Laboratory, Upton, NY 11973, USA.
*Corresponding author. Email: mmitrano@illinois.edu (M.M.); nigel@illinois.edu (N.G.); abbamonte@mrl.illinois.edu (P.A.)
†Present address: MIT Lincoln Laboratory, 244 Wood Street, Lexington, MA 02421, USA.
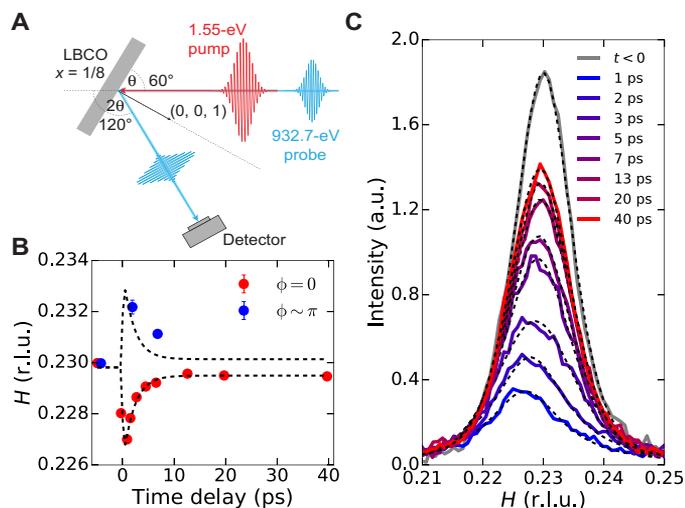‡Present address: Department of Physics, University of Virginia, Charlottesville, VA 22904, USA.

Fig. 1. Pump-induced suppression and recoil of the charge order in LBCO. (**A**) Sketch of the experiment. Pump pulses of 1.55 eV perturb the charge order, which is then probed by resonant scattering of copropagating soft x-ray FEL pulses resonantly tuned to the Cu $L_{3/2}$ edge. In this experiment, there is an additional surface miscut of 21° from the ab plane. (**B**) Time-dependent shift of the charge order wave vector in the H momentum direction for two different azimuthal sample angles, $\phi = 0$ and π. Error bars represent the SD of the pseudo-Voigt peak position fit. The dashed line is a fit to the $\phi = 0$ data (reflected for comparison to the $\phi = \pi$ points) with an exponential function of the type $H(t) = H_0 + \Theta(t)(1 - e^{-t/\tau_0})(\delta He^{-t/\tau} + \delta H_\infty)$ (note S2). (**C**) Transverse momentum scan in the H direction through the charge order peak for a selection of time delays. Dashed lines are fits using a pseudo-Voigt function (note S2). The fluorescence background has been subtracted. a.u., arbitrary units.

Fig. 2. tr-RIXS measurement of charge order in LBCO. (**A**) tr-RIXS spectra taken at a series of delay times, with the momentum tuned to the peak of the charge order, Q_{co} (data are binned in 400-fs time steps to reduce counting noise in the plot). (**B**) Line plots of the same tr-RIXS spectra for a selection of time delays. Error bars represent Poisson counting error. The quasi-elastic scattering from the charge order appears at zero energy and is the only spectral feature influenced by the pump. The feature at −1.8 eV is a combination of dd excitations and Cu^{2+} emission, and the features at −6 eV are charge transfer excitations.

laser (FEL) after a controlled time delay (Fig. 1A). X-ray pulses were resonantly tuned to the Cu $L_{3/2}$ edge (931.5 eV) and detected with either an energy-integrating avalanche photodiode (APD) or an energy-resolving soft x-ray grating spectrometer with a resolution of 0.7 eV (*31, 32*). Using the latter makes this is a time-resolved resonant inelastic x-ray scattering (tr-RIXS) measurement and allows the isolation of the resonant, valence band scattering from the Cu^{2+} fluorescence background. A total delay range of $t_d = 40$ ps after the pump arrival was scanned with a time resolution of $\Delta t = 130$ fs (fig. S1), allowing studies of phenomena with an energy scale ranging from $2\pi\hbar/t_d = 0.103$ meV to $\pi\hbar/\Delta t = 15.9$ meV (*26*).

LBCO is considered the most charge-ordered cuprate. With a correlation length reaching hundreds of lattice parameters, its charge order is often considered "static" (*9, 30*), making it a stringent test case for fluctuating order. Above the transition temperature T_{co}, recent scattering experiments reported evidence of precursory and possibly fluctuating charge order correlations (*33*). The crystal used here orders below $T_{CO} = 53$ K, which coincides with an orthorhombic-to-tetragonal structural transition (*8, 9, 30*). Experiments were carried out at $T = 12$ K, which is above the superconducting $T_c = 5$ K, and focused around the charge order wave vector $\vec{Q}_{CO} = (0.23, 0.00, 1.50)$ reciprocal lattice units (r.l.u.), where (H, K, L) are Miller indices denoting the location of the peak in momentum space (see Materials and Methods for further details) (*9, 30*).

tr-RSXS directly reveals the dynamics of the charge order parameter. A transverse momentum scan through the charge order reflection at a delay time of 1 ps and a pump fluence of 0.1 mJ/cm^2 (Fig. 1C and fig. S3) shows that the peak is suppressed by 75% and broadened in momentum
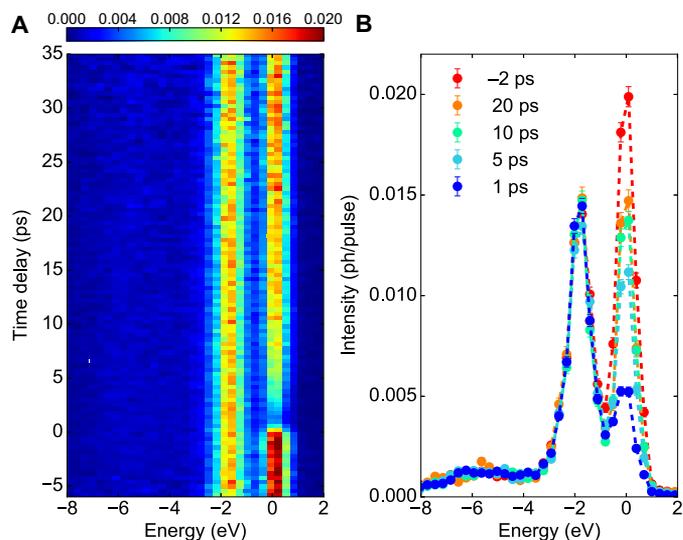
by 45% compared to its equilibrium value, as determined by a pseudo-Voigt fit (note S2) (*34–36*). That the peak is not fully suppressed implies that the laser provided a perturbation of intermediate strength, with which the charge order is not fully extinguished. The broadening of the peak indicates the creation of microscopic heterogeneous structure in the charge order that is transverse in character.

It is crucial to establish whether the peak changes observed are truly properties of the valence band. Repeating the measurement using energy-resolved tr-RIXS with a resolution of 0.7 eV, we find that the peak suppression only takes place in the resonant, quasi-elastic scattering (Fig. 2). The other RIXS features, including the dd and charge transfer excitations and Cu^{2+} fluorescence emission, are unaffected by the pump. We conclude that the effects observed are properties of the valence band and that the time response will directly reveal the dynamics of the charge order.

Shortly after the pump, for time $t \lesssim 2$ ps that corresponds to an energy scale of 2 meV $\lesssim \omega \lesssim$ 15.9 meV, we observe a shift in the wave vector of the charge order peak (see Fig. 1C). This shift occurs in the scattering plane, along the H momentum direction but not along the perpendicular K direction (fig. S2B). A single exponential fit to the time dependence (Fig. 1B) indicates that the peak position recovers in (2.13 ± 0.18) ps. This pump-induced phenomenon could be due to any of three effects: (i) a change in the periodicity of the charge order; (ii) a change in the refractive index of the sample in the soft x-ray regime, which would alter the perceived Bragg angle of the reflection (*37*); or (iii) a collective recoil of the charge order condensate.

We tested the first possibility by rotating the sample azimuthal angle by 180° and repeating the measurement at the same $\vec{Q}_{CO} = (0.23, 0.00, 1.50)$ r.l.u. If the shift were due to a periodicity change, because the CuO_2 plane is C_4 symmetric, then such a rotation would not affect the peak momentum as measured in the reference frame

of the sample. Unexpectedly, we found that the momentum shift reversed direction (Fig. 1B), meaning that it is fixed with respect to the propagation direction of the pump but not the crystal axes. This excludes a (pure) change in the periodicity of the charge order. To test the second possibility, we measured the (0, 0, 1) Bragg reflection of the low-temperature tetragonal structure. A pump-induced change in the refractive index should be visible as a shift in the (0, 0, 1) peak as well; however, no such shift was observed (fig. S6). We are led to the unexpected conclusion that the pump induces a coherent recoil of the charge order condensate—in essence, a nonequilibrium population of collective modes exhibiting a nonzero center-of-mass momentum, which might be thought of as a classical Doppler shift.

After a delay time of 2 ps, the charge order begins to recover. The next stage in its approach to equilibrium is summarized in Fig. 3A, which shows the energy-integrated intensity of the charge order peak for times $2 \text{ ps} \lesssim t \lesssim 10 \text{ ps}$, corresponding to an energy scale of $0.4 \text{ meV} \lesssim \omega \lesssim 2 \text{ meV}$. Unlike previous reports of a gapped amplitude mode (27–29), the recovery of the order parameter is purely exponential, lacking observable oscillations that would indicate inertial dynamics. This observation is unexpected because a conventional charge density wave (CDW) is normally gapped either by the crystal lattice or by disorder, resulting in inertial dynamics (38–40). It also is at odds with evidence from previous optics experiments that do not directly probe the charge order parameter (27–29). We conclude that the transverse dynamics in LBCO, previously thought to exhibit static charge order, are relaxational, meaning that the transverse excitations are gapless and will fluctuate at any finite temperature.

The momentum dependence of the charge order dynamics reveals that the collective excitations propagate by Brownian diffusion. In the standard description of relaxational dynamics in a periodic system (note S7) (24, 25, 41–44), a nonconserved order parameter driven weakly out of equilibrium will have a time dependence proportional to $\exp[-\gamma(q)t]$, where $q = |\vec{Q} - \vec{Q}_{CO}|$ is the momentum relative to the charge order peak and

$$\gamma(q) = \gamma_0 + Dq^2 \qquad (1)$$

Here, γ_0 describes pure dissipation, and the momentum dependence arises from diffusion quantified by the parameter, D. Figure 3A shows time traces of the charge order peak intensity for $t < 10 \text{ ps}$ and for a selection of momenta $\vec{Q}$ along the transverse direction around $\vec{Q}_{CO}$. Each curve is fit well by a single exponential function and a constant offset that likely arises from heating of the electronic subsystem (note S6) (45). The exponential behavior is consistent with the charge order deviating only slightly from its equilibrium value (24, 25). We find that the relaxation rate is highly momentum dependent, increasing rapidly with q (Fig. 3B), and is fit well by Eq. 1, yielding dissipation parameter $\hbar\gamma_0 = (0.1730 \pm 0.0015) \text{ meV}$ and diffusion constant $\hbar D = (215 \pm 19) \text{ meV Å}^2$. These two quantities imply that the transverse collective excitations of the charge order in LBCO propagate by diffusion, with a characteristic diffusion length $\lambda = \sqrt{2D/\gamma_0} = (49.9 \pm 2.2) \text{ Å}$ and dissipation time $1/\gamma_0 = (3.805 \pm 0.031) \text{ ps}$. Notably, the characteristic charge order fluctuation energy $\gamma_0 \sim 2 \text{ K}$ is similar to the superconducting T_c at $x \sim 1/8$, thus suggesting a connection between the two phenomena.

At late times, $5 \text{ ps} \lesssim t \lesssim 40 \text{ ps}$, corresponding to an energy scale of $0.1 \text{ meV} \lesssim \omega \lesssim 0.8 \text{ meV}$, the order parameter amplitude is close to its equilibrium value. The dynamics no longer follow a simple exponential function but instead are characterized by self-similar dynamic scaling (46–49). The concept of dynamic scaling originated in the field of far-from-equilibrium phenomena having been observed in phase-ordering dynamics of quenched binary fluids and alloys (50, 51). The hypothesis states that the amplitude and length scale of the order parameter satisfy a universal relationship

$$S(q, t) = L^d(t)F[qL(t)] \qquad (2)$$

Here, $S(q, t)$ is the time Fourier transform of $S(q, \omega)$, $L(t)$ is the characteristic length scale of the order, and $F(x)$ is a universal function. For systems with a scalar order parameter, L corresponds to the mean domain size. For systems with a continuous symmetry and a vector or tensor order parameter, $L(t)$ corresponds to the mean distance between topological defects and increases as defects annihilate or are annealed from the system. Equation 2 states that the fluctuations are self-similar and independent of time if suitably scaled. Dynamic scaling only takes place at late times following a quench when the magnitude of the order parameter is large and nonlinear effects are important (47, 52).

Using Eq. 2, the late-time data collapse to a single curve (Fig. 4A) when taking $d = 3$ and defining $L(t)$ as the inverse of the half-width of the charge order reflection. This collapse implies that, at sub–millielectron volt energy scales, the transverse dynamics of the order parameter are determined by universal properties such as dimensionality and ranges of the interactions and are not governed by the microscopic details of LBCO itself.

The behavior of $L(t)$ is sensitive to the nature of the equilibrium phase that the system is approaching. If relaxing to a phase that is uniform in space, then $L(t)$ is known to exhibit power law behavior at
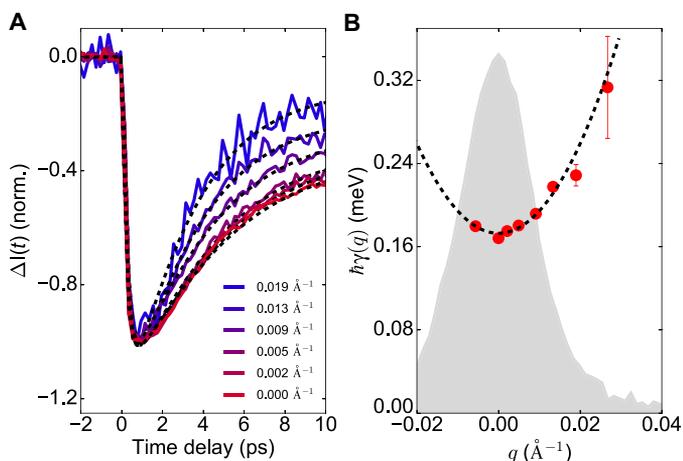

Fig. 3. Collective modes of charge order in LBCO propagate diffusively. (**A**) Solid lines: Time traces of the energy-integrated charge order scattering for a selection of momenta $q = |\vec{Q} - \vec{Q}_{CO}|$. The data are scaled to the same height and binned into 200-fs time steps to reduce counting noise in the plot. Dashed lines: Fits using a single exponential function (see note S6) show that the recovery time is highly momentum dependent. (**B**) Red points: Exponential decay parameter, $\gamma(q)$, as a function of relative momentum difference, $q = \text{sgn}(H - H_{CO})|\vec{Q} - \vec{Q}_{CO}|$. Error bars represent only the statistical uncertainties in the fits. Dashed line: Fit to the data using Eq. 1. Shaded area: Line shape of the unperturbed charge order reflection in equilibrium.
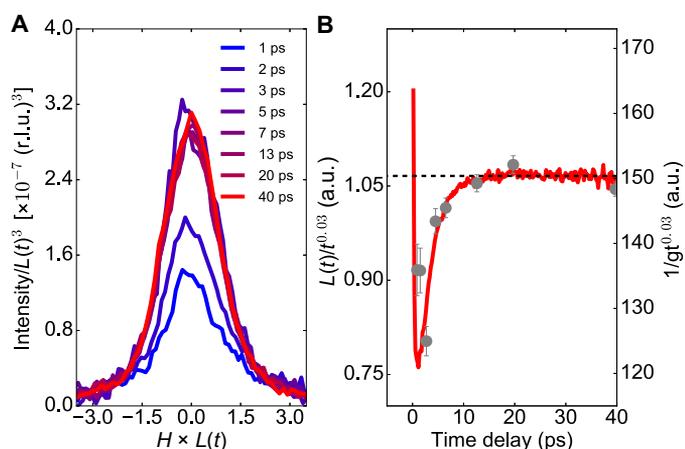
Fig. 4. Demonstration of dynamic scale invariance at long times. (A) Scaled momentum profiles (as in Fig. 1C) showing that the data collapse at late times for $d = 3$. Here, $L(t)$ is taken to be the inverse half-width of the reflection at each time delay, t. The curves have been shifted in H to compensate for the momentum recoil at short times. **(B)** Compensated plot of the scaling function, $L(t)$, taken to be the inverse half-width $1/g$ of the order parameter reflection (gray circles) or the cube root of the peak intensity at each time delay, t, i.e., by inverting the dynamical scaling relation $S(0, t) = L^3(t)F(0)$ (red line). The data show a power law of 0.03 at long times, indicating a logarithmic behavior.

long times, $L(t) \sim t^{\alpha}$, where $\alpha = 1/3$ if the order parameter is conserved and $\alpha = 1/2$ if it is not (46, 47). If the equilibrium phase is modulated, as is the current case of charge order in LBCO, it was predicted (for a strong quench) that the long-time behavior of two-dimensional (2D) modulated phase order is governed by the dynamics of topological defects, and $L(t) \sim \ln (t)$ (53). These slow dynamics can arise without needing to consider additional effects due to pinning by disorder. That neighboring layers are correlated means that the topological defects behave as line defects oriented along the stacking direction and so can be described by an effective 2D dynamics.

We test these expectations by examining the long-time ($t > 10$ ps) behavior of $L(t)$. Figure 4B shows a compensated plot seemingly indicating that $L(t) \sim t^{0.03}$ at long times. Small power laws of this sort are normally interpreted as logarithmic dependence, i.e., $L(t) \sim \ln (t)$, supporting the prediction of Hou et al. (53). While disorder may be playing some role, this result is evidence that the long-time dynamics of LBCO are governed by the propagation of a dilute concentration of topological defects that are transverse in nature, such as dislocation lines. The functional form of the thermalization process of the charge-ordered phase, characterized by the presence of dynamical scaling phenomena and of diffusive behavior, is independent of the sample temperature well below the critical point.

CONCLUSION
Our results show that the charge order in LBCO is dynamic, undergoing transverse fluctuations at millielectron volt energy scales. On an energy scale of 0.4 to 2 meV, the dynamics are relaxational, meaning that the collective excitations are gapless and propagate by diffusion. This conclusion is based on the direct measurement of the charge order parameter. The gapless nature of the charge order is unexpected because a conventional CDW is normally gapped by pinning on the lattice (e.g., to the LBCO low-temperature tetragonal distortion) or impurities (38–40, 54) and suggests that these fluctuations are a pre-

viously unidentified property specific to the cuprates. The energy scale of the transverse fluctuations is comparable to the superconducting energy, $k_B T_c$, suggesting a connection to superconductivity and supporting arguments that transverse stripe fluctuations might modulate the interstripe Josephson coupling (1). At ultralow-energy scales, <0.4 meV, the charge order exhibits dynamic critical scaling, indicating that the dynamics are determined by the universal propagation of transverse topological defects (53), e.g., dislocations in the charge order. Our study establishes tr-RSXS as a new tool to study collective charge dynamics of quantum materials at yet unexplored low-energy scales.

MATERIALS AND METHODS
Sample growth and characterization
A high-quality pellet of $La_{1.875}Ba_{0.125}CuO_4$ was grown by the floating zone method and cut into smaller single crystals (30). The crystals were cleaved in air to expose a fresh surface, mainly oriented along the ab plane. The 2-mm–sized single crystal used in this study was preoriented using a laboratory-based $CuK\alpha$ x-ray source. The lattice parameters were determined to be $a = b = 3.787$ Å and $c = 13.23$ Å. The surface miscut with respect to the ab crystalline plane was found to be 21°. The superconducting T_c of the sample was verified through a SQUID (superconducting quantum interference device) magnetometry measurement to be approximately 5 K.

Time-resolved resonant soft x-ray scattering
Low-temperature optical pump, soft x-ray probe measurements were performed at the Soft X-Ray (SXR) instrument of the Linac Coherent Light Source (LCLS) X-ray FEL at SLAC National Laboratory, Menlo Park, USA (55). The measurements reported in this work were carried out at an RSXS endstation (31) in a vacuum of 3×10^{-9} torr. Low temperatures down to 12 K were achieved with a manipulator equipped with a Helium flow cryostat. Ultrafast probe x-rays at a repetition rate of 120 Hz were obtained by tuning the FEL to the Cu $L_{3/2}$ edge (931.5 eV) and with a bandwidth of 0.3 eV after passing through a grating monochromator. The p-polarized x-ray pulses had a typical pulse duration of 60 fs and a pulse energy of 1.5 µJ and were focused down to an elliptical spot of 1.5×0.03 mm². The optical pump pulses of 1.55 eV, also p-polarized, were generated with a Ti:sapphire amplifier run at 120 Hz and propagated collinearly with the x-rays into the RSXS endstation. The 50-fs pump was focused down to a spot of 2.0×1.0 mm² to probe a homogeneously excited sample volume. The beams were spatially overlapped onto a frosted Ce:YAG crystal and synchronized by monitoring the reflectivity changes of a Si_3N_4 thin film. The shot-to-shot temporal jitter between pump and probe pulses was measured by means of a timing tool (56, 57) and corrected by time sorting during the data analysis. The overall time resolution of approximately 130 fs was checked by measuring the cross-correlation signal on a polished Ce:YAG crystal (see fig. S1). Shot-to-shot intensity fluctuations from the FEL were corrected in the photodiode data through a reference intensity readout before the monochromator. The scattered x-rays were measured with an energy-integrating APD located on a rotating arm at 17.3 cm from the sample, while tr-RIXS measurements were performed with a modular qRIXS grating spectrometer (32) mounted on a port at 135° with respect to the incident beam and provided an energy resolution of ~0.7 eV (full width at half maximum) when using the second order of the grating. The spectrometer was equipped with an ANDOR charge-coupled device camera operated at a readout rate of 120 Hz in 1D binning mode along the nondispersive direction. The

pump-probe time delay was controlled both electronically and through a mechanical translation stage. All the time-dependent rocking curves presented in this work were referenced to their equilibrium values by selectively varying the pump-probe time delay to negative values during the data acquisition to minimize errors due to motor backlash and step accuracy.

SUPPLEMENTARY MATERIALS

Supplementary material for this article is available at http://advances.sciencemag.org/cgi/content/full/5/8/eaax3346/DC1

Note S1. Pump-probe cross-correlation
Note S2. Charge order peak rocking curves fit and background subtraction
Note S3. Charge order peak rocking curves for $\phi \sim \pi$
Note S4. Comparison between tr-RIXS and APD data
Note S5. Response of the low-temperature tetragonal distortion peak
Note S6. Raw time-dependent, energy-integrated peak intensities around Q_{CO}
Note S7. Momentum-dependent recovery of the charge-ordered phase
Fig. S1. Optical pump x-ray probe cross-correlation.
Fig. S2. Pump-induced CO peak melting.
Fig. S3. Time-dependent CO peak fit parameters.
Fig. S4. CO peak shift at $\phi \sim \pi$.
Fig. S5. Comparison between tr-RIXS and energy-integrated time dependence at Q_{co}.
Fig. S6. Dynamics of the low-temperature tetragonal distortion.
Fig. S7. Raw time-dependent CO peak intensity.
Fig. S8. Schematic representation of the scattering geometry.
Table S1. Fit parameters along K projection.

REFERENCES AND NOTES

1. S. A. Kivelson, E. Fradkin, V. J. Emery, Electronic liquid-crystal phases of a doped mott insulator. *Nature* **393**, 550–553 (1998).
2. M. Vojta, Lattice symmetry breaking in cuprate superconductors: Stripes, nematics, and superconductivity. *Adv. Phys.* **58**, 699–820 (2009).
3. B. Keimer, S. A. Kivelson, M. R. Norman, S. Uchida, J. Zaanen, From quantum matter to high-temperature superconductivity in copper oxides. *Nature* **518**, 179–186 (2015).
4. J. G. Bednorz, K. A. Müller, Possible high T_c superconductivity in the Ba–La–Cu–O system. *Z. Phys. B: Condens. Matter* **64**, 189–193 (1986).
5. K. Machida, Magnetism in La_2CuO_4 based compounds. *Physica C* **158**, 192–196 (1989).
6. H. J. Schulz, Domain walls in a doped antiferromagnet. *J. Phys. France* **50**, 2833–2849 (1989).
7. J. Zaanen, O. Gunnarsson, Charged magnetic domain lines and the magnetism in high-T_c oxides. *Phys. Rev. B* **40**, R7391–R7394 (1989).
8. J. M. Tranquada, H. Woo, T. G. Perring, H. Goka, G. D. Gu, G. Xu, M. Fujita, K. Yamada, Quantum magnetic excitations from stripes in copper oxide superconductors. *Nature* **429**, 534–538 (2004).
9. P. Abbamonte, A. Rusydi, S. Smadici, G. D. Gu, G. A. Sawatzky, D. L. Feng, Spatially modulated 'Mottness' in $La_{2-x}Ba_xCuO_4$. *Nat. Phys.* **1**, 155–158 (2005).
10. S. A. Kivelson, E. Fradkin, *Handbook of High-Temperature Superconductivity*, J. R. Schrieffer, J. S. Brooks, Eds. (Springer Science, 2007), chap. 15, pp. 570–592.
11. G. Ghiringhelli, M. Le Tacon, M. Minola, S. Blanco-Canosa, C. Mazzoli, N. B. Brookes, G. M. De Luca, A. Frano, D. G. Hawthorn, F. He, T. Loew, M. M. Sala, D. C. Peets, M. Salluzzo, E. Schierle, R. Sutarto, G. A. Sawatzky, E. Weschke, B. Keimer, L. Braicovich, Long-range incommensurate charge fluctuations in (Y,Nd)$Ba_2Cu_3O_{6+x}$. *Science* **337**, 821–825 (2012).
12. R. Comin, A. Frano, M. M. Yee, Y. Yoshida, H. Eisaki, E. Schierle, E. Weschke, R. Sutarto, F. He, A. Soumyanarayanan, Y. He, M. Le Tacon, I. S. Elfimov, J. E. Hoffman, G. A. Sawatzky, B. Keimer, A. Damascelli, Charge order driven by Fermi-arc instability in $Bi_2Sr_{2-x}La_xCuO_{6+\delta}$. *Science* **343**, 390–392 (2014).
13. E. H. da Silva Neto, P. Aynajian, A. Frano, R. Comin, E. Schierle, E. Weschke, A. Gyenis, J. Wen, J. Schneeloch, Z. Xu, S. Ono, G. Gu, M. Le Tacon, A. Yazdani, Ubiquitous interplay between charge ordering and high-temperature superconductivity in cuprates. *Science* **343**, 393–396 (2014).
14. M. Le Tacon, A. Bosak, S. M. Souliou, G. Dellea, T. Loew, R. Heid, K.-P. Bohnen, G. Ghiringhelli, M. Krisch, B. Keimer, Inelastic x-ray scattering in $YBa_2Cu_3O_{6.6}$ reveals giant phonon anomalies and elastic central peak due to charge-density-wave formation. *Nat. Phys.* **10**, 52–58 (2014).
15. J. Chang, E. Blackburn, A. T. Holmes, N. B. Christensen, J. Larsen, J. Mesot, R. Liang, D. A. Bonn, W. N. Hardy, A. Watenphul, M. von Zimmermann, E. M. Forgan, S. M. Hayden, Direct observation of competition between superconductivity and charge density wave order in $YBa_2Cu_3O_{6.67}$. *Nat. Phys.* **8**, 871–876 (2012).
16. E. Berg, E. Fradkin, S. A. Kivelson, Theory of the striped superconductor. *Phys. Rev. B* **79**, 064515 (2009).
17. E. Fradkin, S. A. Kivelson, J. M. Tranquada, *Colloquium*: Theory of intertwined orders in high temperature superconductors. *Rev. Mod. Phys.* **87**, 457–482 (2015).
18. S. Gerber, H. Jang, H. Nojiri, S. Matsuzawa, H. Yasumura, D. A. Bonn, R. Liang, W. N. Hardy, Z. Islam, A. Mehta, S. Song, M. Sikorski, D. Stefanescu, Y. Feng, S. A. Kivelson, T. P. Devereaux, Z.-X. Shen, C. C. Kao, W. S. Lee, D. Zhu, J. S. Lee, Three-dimensional charge density wave order in $YBa_2Cu_3O_{6.67}$ at high magnetic fields. *Science* **350**, 949–952 (2015).
19. M. H. Hamidian, S. D. Edkins, S. H. Joo, A. Kostin, H. Eisaki, S. Uchida, M. J. Lawler, E. A. Kim, A. P. Mackenzie, K. Fujita, J. Lee, J. C. S. Davis, Detection of a Cooper-pair density wave in $Bi_2Sr_2CaCu_2O_{8+x}$. *Nature* **532**, 343–347 (2016).
20. S. A. Kivelson, I. P. Bindloss, E. Fradkin, V. Oganesyan, J. M. Tranquada, A. Kapitulnik, C. Howald, How to detect fluctuating stripes in the high-temperature superconductors. *Rev. Mod. Phys.* **75**, 1201–1241 (2003).
21. E. Berg, E. Fradkin, E.-A. Kim, S. A. Kivelson, V. Oganesyan, J. M. Tranquada, S. C. Zhang, Dynamical layer decoupling in a stripe-ordered high-T_c superconductor. *Phys. Rev. Lett.* **99**, 127003 (2007).
22. D. Pines, P. Noziéres, *The Theory of Quantum Liquids*, Advanced Book Classics (Perseus Books, 1966).
23. L. D. Landau, E. M. Lifshitz, *Physical Kinetics*, Course of Theoretical Physics (Pergamon Press Ltd., 1981).
24. N. Goldenfeld, *Lectures on Phase Transitions and the Renormalization Group*, Frontiers in Physics (Westview Press, 1992).
25. P. M. Chaikin, T. C. Lubensky, *Principles of Condensed Matter Physics* (Cambridge University Press, 1995).
26. P. Abbamonte, T. Graber, J. P. Reed, S. Smadici, C.-L. Yeh, A. Shukla, J.-P. Rueff, W. Ku, Dynamical reconstruction of the exciton in LiF with inelastic x-ray scattering. *Proc. Natl. Acad. Sci. U.S.A.* **105**, 12159–12163 (2008).
27. D. H. Torchinsky, F. Mahmood, A. T. Bollinger, I. Božović, N. Gedik, Fluctuating charge-density waves in a cuprate superconductor. *Nat. Mater.* **12**, 387–391 (2013).
28. G. L. Dakovski, W.-S. Lee, D. G. Hawthorn, N. Garner, D. Bonn, W. Hardy, R. Liang, M. C. Hoffmann, J. J. Turner, Enhanced coherent oscillations in the superconducting state of underdoped $YBa_2Cu_3O_{6+x}$ induced via ultrafast terahertz excitation. *Phys. Rev. B* **91**, 220506 (2015).
29. J. P. Hinton, J. D. Koralek, Y. M. Lu, A. Vishwanath, J. Orenstein, D. A. Bonn, W. N. Hardy, R. Liang, New collective mode in $YBa_2Cu_3O_{6+x}$ observed by time-domain reflectometry. *Phys. Rev. B* **88**, 060508 (2013).
30. M. Hücker, M. von Zimmermann, G. D. Gu, Z. J. Xu, J. S. Wen, G. Xu, H. J. Kang, A. Zheludev, J. M. Tranquada, Stripe order in superconducting $La_{2-x}Ba_xCuO_4$ ($0.095 \leq x \leq 0.155$). *Phys. Rev. B* **83**, 104506 (2011).
31. D. Doering, Y.-D. Chuang, N. Andresen, K. Chow, D. Contarato, C. Cummings, E. Domning, J. Joseph, J. S. Pepper, B. Smith, G. Zizka, C. Ford, W. S. Lee, M. Weaver, L. Patthey, J. Weizeorick, Z. Hussain, P. Denes, Development of a compact fast CCD camera and resonant soft x-ray scattering endstation for time-resolved pump-probe experiments. *Rev. Sci. Instrum.* **82**, 073303–073309 (2011).
32. Y. D. Chuang, Y. C. Shao, A. Cruz, K. Hanzel, A. Brown, A. Frano, R. Qiao, B. Smith, E. Domning, S. W. Huang, L. A. Wray, W. S. Lee, Z.-X. Shen, T. P. Devereaux, J.-W. Chiou, W.-F. Pong, V. V. Yashchuk, E. Gullikson, R. Reininger, W. Yang, J. Guo, R. Duarte, Z. Hussain, Modular soft x-ray spectrometer for applications in energy sciences and quantum materials. *Rev. Sci. Instrum.* **88**, 013110 (2017).
33. H. Miao, J. Lorenzana, G. Seibold, Y. Y. Peng, A. Amorese, F. Yakhou-Harris, K. Kummer, N. B. Brookes, R. M. Konik, V. Thampy, G. D. Gu, G. Ghiringhelli, L. Braicovich, M. P. M. Dean, High-temperature charge density wave correlations in $La_{1.875}Ba_{0.125}CuO_4$ without spin-charge locking. *Proc. Natl. Acad. Sci. U.S.A.* **114**, 12430–12435 (2017).
34. M. Först, R. I. Tobey, H. Bromberger, S. B. Wilkins, V. Khanna, A. D. Caviglia, Y. D. Chuang, W. S. Lee, W. F. Schlotter, J. J. Turner, M. P. Minitti, O. Krupin, Z. J. Xu, J. S. Wen, G. D. Gu, S. S. Dhesi, A. Cavalleri, J. P. Hill, Melting of charge stripes in vibrationally driven $La_{1.875}Ba_{0.125}CuO_4$: Assessing the respective roles of electronic and lattice order in frustrated superconductors. *Phys. Rev. Lett.* **112**, 157002 (2014).
35. V. Khanna, R. Mankowsky, M. Petrich, H. Bromberger, S. A. Cavill, E. Möhr-Vorobeva, D. Nicoletti, Y. Laplace, G. D. Gu, J. P. Hill, M. Först, A. Cavalleri, S. S. Dhesi, Restoring interlayer josephson coupling in $La_{1.885}Ba_{0.115}CuO_4$ by charge transfer melting of stripe order. *Phys. Rev. B* **93**, 224522 (2016).
36. W. S. Lee, Y. D. Chuang, R. G. Moore, Y. Zhu, L. Patthey, M. Trigo, D. H. Lu, P. S. Kirchmann, O. Krupin, M. Yi, M. Langner, N. Huse, J. S. Robinson, Y. Chen, S. Y. Zhou, G. Coslovich, B. Huber, D. A. Reis, R. A. Kaindl, R. W. Schoenlein, D. Doering, P. Denes, W. F. Schlotter, J. J. Turner, S. L. Johnson, M. Först, T. Sasagawa, Y. F. Kung, A. P. Sorini, A. F. Kemper, B. Moritz, T. P. Devereaux, D.-H. Lee, Z.-X. Shen, Z. Hussain, Phase fluctuations and the absence of topological defects in a photo-excited charge-ordered nickelate. *Nat. Commun.* **3**, 838 (2012).
37. S. Smadici, J. C. T. Lee, S. Logvenov, I. Bozovic, P. Abbamonte, Form factor dispersion at La $M_{5,4}$ edges and average density of resonant atoms. *J. Phys. Condens. Matter* **26**, 025303 (2013).

38. T. Huber, S. O. Mariager, A. Ferrer, H. Schäfer, J. A. Johnson, S. Grübel, A. Lübcke, L. Huber, T. Kubacka, C. C. Dornes, C. Laulhe, S. Ravy, G. Ingold, P. Beaud, J. Demsar, S. L. Johnson, Coherent structural dynamics of a prototypical charge-density-wave-to-metal transition. *Phys. Rev. Lett.* **113**, 026401 (2014).

39. P. Beaud, A. Caviezel, S. O. Mariager, L. Rettig, G. Ingold, C. Dornes, S.-W. Huang, J. A. Johnson, M. Radovic, T. Huber, T. Kubacka, A. Ferrer, H. T. Lemke, M. M. Chollet, D. Zhu, J. M. Glownia, M. Sikorski, A. Robert, H. Wadati, M. Nakamura, M. Kawasaki, Y. Tokura, S. L. Johnson, U. U. Staub, A time-dependent order parameter for ultrafast photoinduced phase transitions. *Nat. Mater.* **13**, 923–927 (2014).

40. G. Grüner, *Density Waves in Solids, Frontiers in Physics* (Perseus Books, 1994).

41. J. Swift, P. C. Hohenberg, Hydrodynamic fluctuations at the convective instability. *Phys. Rev. A* **15**, 319–328 (1977).

42. M. Cross, P. Hohenberg, Pattern formation outside of equilibrium. *Rev. Mod. Phys.* **65**, 851–1112 (1993).

43. M. Karttunen, M. Haataja, K. Elder, M. Grant, Defects, order, and hysteresis in driven charge-density waves. *Phys. Rev. Lett.* **83**, 3518–3521 (1999).

44. A. Newell, J. Whitehead, Finite bandwidth, finite amplitude convection. *J. Fluid Mech.* **38**, 279–303 (1969).

45. L. Perfetti, P. A. Loukakos, M. Lisowski, U. Bovensiepen, H. Eisaki, M. Wolf, Ultrafast electron relaxation in superconducting $Bi_2Sr_2CaCu_2O_{8+\delta}$ by time-resolved photoelectron spectroscopy. *Phys. Rev. Lett.* **99**, 197001 (2007).

46. A. J. Bray, Theory of phase ordering kinetics. *Adv. Phys.* **43**, 357 (1994).

47. M. Mondello, N. D. Goldenfeld, Scaling and vortex dynamics after the quench of a system with a continuous symmetry. *Phys. Rev. A* **42**, 5865–5872 (1990).

48. M. Mondello, N. D. Goldenfeld, Scaling and vortex-string dynamics in a three-dimensional system with a continuous symmetry. *Phys. Rev. A* **45**, 657–664 (1992).

49. S. Vogelgesang, G. Storeck, J. G. Horstmann, T. Diekmann, M. Sivis, S. Schramm, K. Rossnagel, S. Schäfer, C. Ropers, Phase ordering of charge density waves traced by ultrafast low-energy electron diffraction. *Nat. Phys.* **14**, 184–190 (2018).

50. Y. C. Chou, I. Goldburg, Angular distribution of light scattered from critically quenched liquid mixtures. *Phys. Rev. A* **23**, 858–864 (1981).

51. B. D. Gaulin, S. Spooner, Y. Morii, Kinetics of phase separation in $Mn_{0.67}Cu_{0.33}$. *Phys. Rev. Lett.* **59**, 668–671 (1987).

52. T. Nagaya, H. Orihara, Y. Ishibashi, Coarsening dynamics of +1 and -1 disclinations in two-dimensionally aligned nematics –spatial distribution of disclinations. *J. Physical Soc. Japan* **64**, 78–85 (1995).

53. Q. Hou, S. Sasa, N. Goldenfeld, Dynamical scaling behavior of the swift-hohenberg equation following a quench to the modulated state. *Physica A: Stat. Mech. Appl.* **239**, 219–226 (1997).

54. X. M. Chen, C. Mazzoli, Y. Cao, V. Thampy, A. M. Barbour, W. Hu, M. Lu, T. A. Assefa, H. Miao, G. Fabbris, G. D. Gu, J. M. Tranquada, M. P. M. Dean, S. B. Wilkins, I. K. Robinson, Charge density wave memory in a cuprate superconductor. *Nat. Commun.* **10**, 1435 (2019).

55. W. F. Schlotter, J. J. Turner, M. Rowen, P. Heimann, M. Holmes, O. Krupin, M. Messerschmidt, S. Moeller, J. Krzywinski, R. Soufli, M. Fernández-Perea, N. Kelez, S. Lee, R. Coffee, G. Hays, M. Beye, N. Gerken, F. Sorgenfrei, S. Hau-Riege, L. Juha, J. Chalupsky, V. Hajkova, A. P. Mancuso, A. Singer, O. Yefanov, I. A. Vartanyants, G. Cadenazzi, B. Abbey, K. A. Nugent, H. Sinn, J. Lüning, S. Schaffert, S. Eisebitt, W. S. Lee, A. Scherz, A. R. Nilsson, W. Wurth, The soft x-ray instrument for materials studies at the Linac Coherent Light Source x-ray free-electron laser. *Rev. Sci. Instrum.* **83**, 043107 (2012).

56. H. T. Lemke, M. Weaver, M. Chollet, J. Robinson, J. M. Glownia, D. Zhu, M. R. Bionta, M. Cammarata, M. Harmand, R. N. Coffee, D. M. Fritz, *SPIE Optics + Optoelectronics*, T. Tschentscher, K. Tiedtke, Eds. (SPIE, 2013), pp. 87780S–5.

57. M. Harmand, R. Coffee, M. R. Bionta, M. Chollet, D. French, D. Zhu, D. M. Fritz, H. T. Lemke, N. Medvedev, B. Ziaja, S. Toleikis, M. Cammarata, Achieving few-femtosecond time-sorting at hard x-ray free-electron lasers. *Nat. Photonics* **7**, 215–218 (2013).

Science Advances

Ultrafast time-resolved x-ray scattering reveals diffusive charge order dynamics in La$_{2-x}$Ba$_x$CuO$_4$

Matteo Mitrano, Sangjun Lee, Ali A. Husain, Luca Delacretaz, Minhui Zhu, Gilberto de la Peña Munoz, Stella X.-L. Sun, Young Il Joe, Alexander H. Reid, Scott F. Wandel, Giacomo Coslovich, William Schlotter, Tim van Driel, John Schneeloch, G. D. Gu, Sean Hartnoll, Nigel Goldenfeld and Peter Abbamonte

ARTICLE TOOLS	http://advances.sciencemag.org/content/5/8/eaax3346
SUPPLEMENTARY MATERIALS	http://advances.sciencemag.org/content/suppl/2019/08/12/5.8.eaax3346.DC1
REFERENCES	This article cites 50 articles, 6 of which you can access for free http://advances.sciencemag.org/content/5/8/eaax3346#BIBL
PERMISSIONS	http://www.sciencemag.org/help/reprints-and-permissions

Use of this article is subject to the Terms of Service